

Supporting Information For:

Targeted polymersome delivery of a stapled peptide for drugging the tumor protein p53:BCL-2-family axis in diffuse large B-cell lymphoma

Mathew R. Schnorenberg^{1,2,3}, Katrina M. Hawley², Anika T. Thomas-Toth², Elyse A. Watkins¹, Yu Tian^{1,2}, Jeffrey M. Ting¹, Logan B. Leak², Isadora M. Kucera^{1,2}, Michal M. Raczy¹, Andrew L. Kung⁴, Jeffrey A. Hubbell¹, Matthew V. Tirrell^{1,}, James L. LaBelle^{2,*}*

¹Pritzker School of Molecular Engineering, University of Chicago, Chicago, IL 60637, USA.

²Department of Pediatrics, Section of Hematology/Oncology, University of Chicago, Chicago, IL 60637, USA.

³Medical Scientist Training Program, Pritzker School of Medicine, University of Chicago, Chicago, IL 60637, USA.

⁴Department of Pediatrics, Memorial Sloan Kettering Cancer Center, New York, NY 10065, USA.

*Corresponding Authors:

James L. LaBelle
900 East 57th Street, KCBD 5122
Chicago, IL 60637
Email: jlabelle@peds.bsd.uchicago.edu
Phone: 773-702-6812
Fax: 773-834-1329

Matthew V. Tirrell
Pritzker School of Molecular Engineering
5640 South Ellis Avenue
Chicago, IL 60637
Email: mtirrell@uchicago.edu
Phone: 773-834-2001
Fax: 773-834-7756

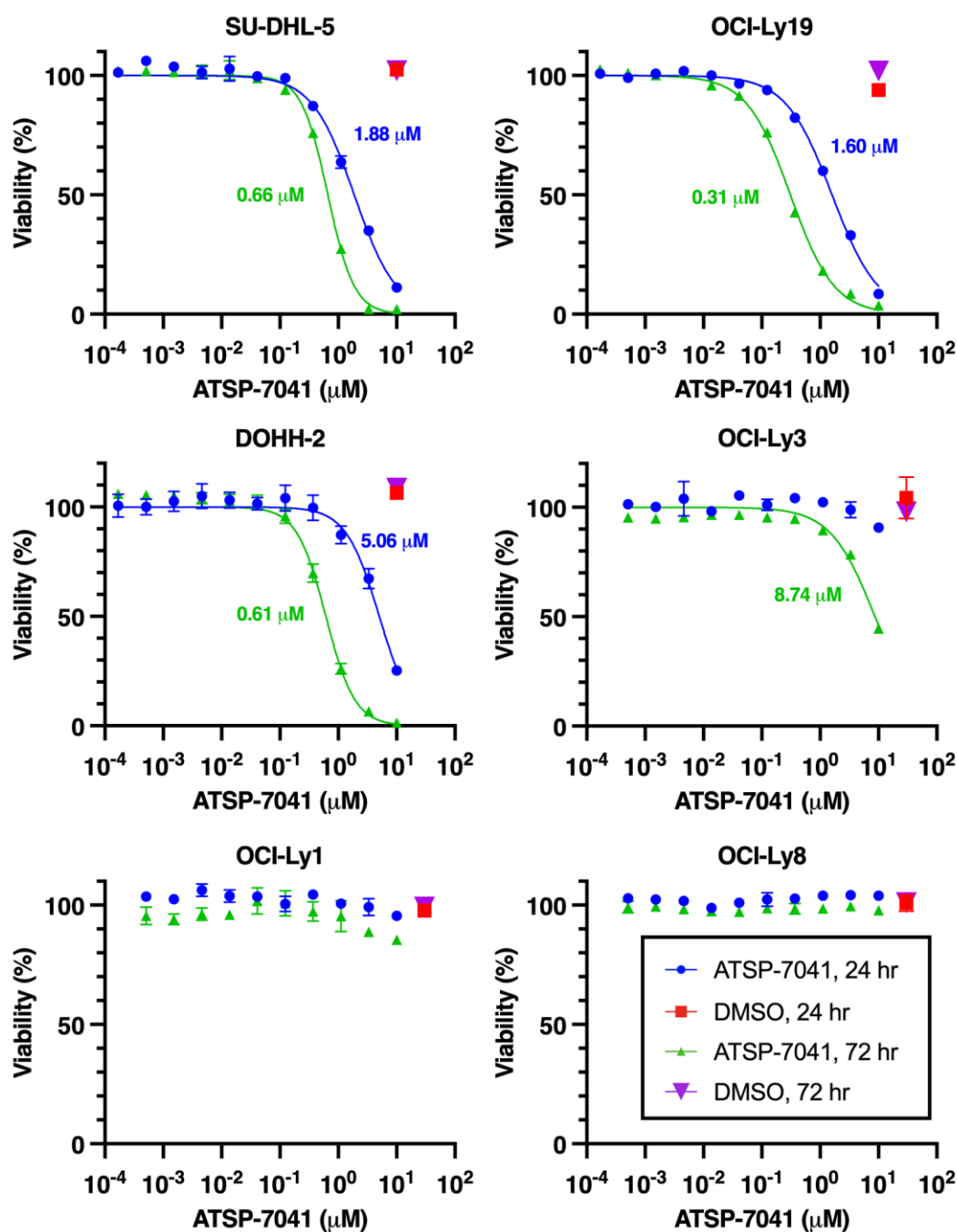


Figure S1: DLBCL cell death sensitivity to ATSP-7041. DLBCL cell lines were treated with ATSP-7041 or DMSO vehicle for 24 or 72 hr, and viability was measured. Data were normalized to untreated cells from the same time point, plotted as the mean of duplicates \pm SEM, and fitted using nonlinear regression. EC₅₀ is shown. Any absent error bars are smaller than the plotted point.

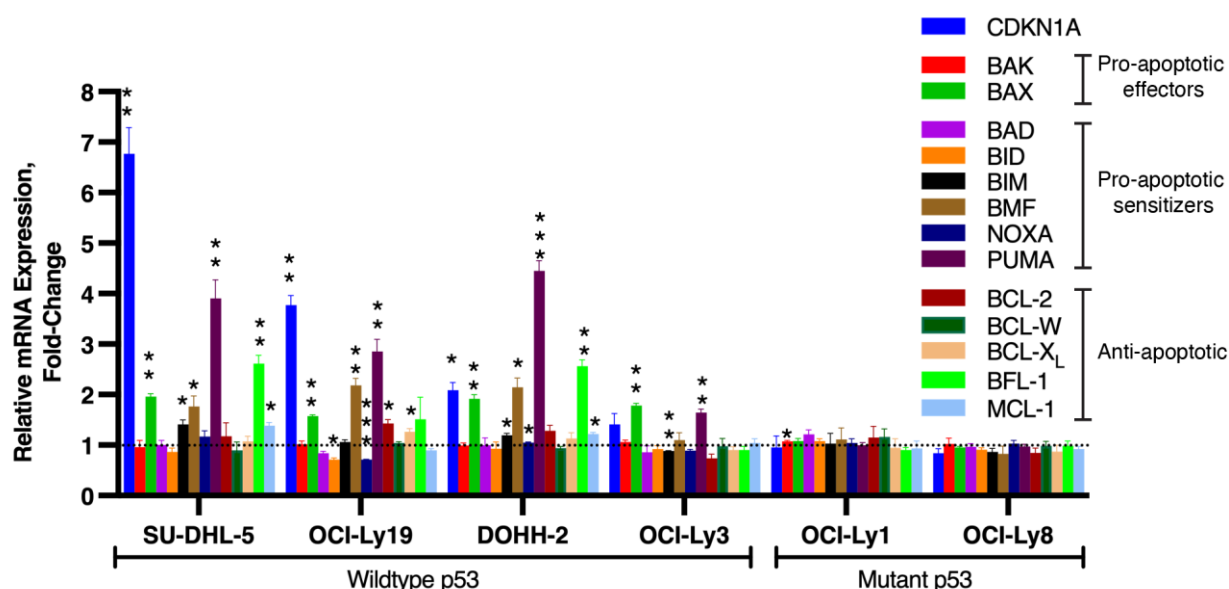


Figure S2: Changes in mRNA expression of the BCL-2 family in response to p53-reactivation by ATSP-7041. DLBCL cell lines were treated with 1 μ M ATSP-7041 for 24 hr, and mRNA changes in the BCL-2 family were measured by qRT-PCR. Plotted values are the mean of the relative fold change of biological triplicates \pm SEM, using GAPDH and B2M as housekeeping genes and DMSO-treated samples as reference controls. Changes were deemed significant via one-sample t-test ($H_0: \Delta\Delta CT = 0$; * $p < 0.05$, ** $p < 0.01$, *** $p < 0.001$, **** $p < 0.0001$).

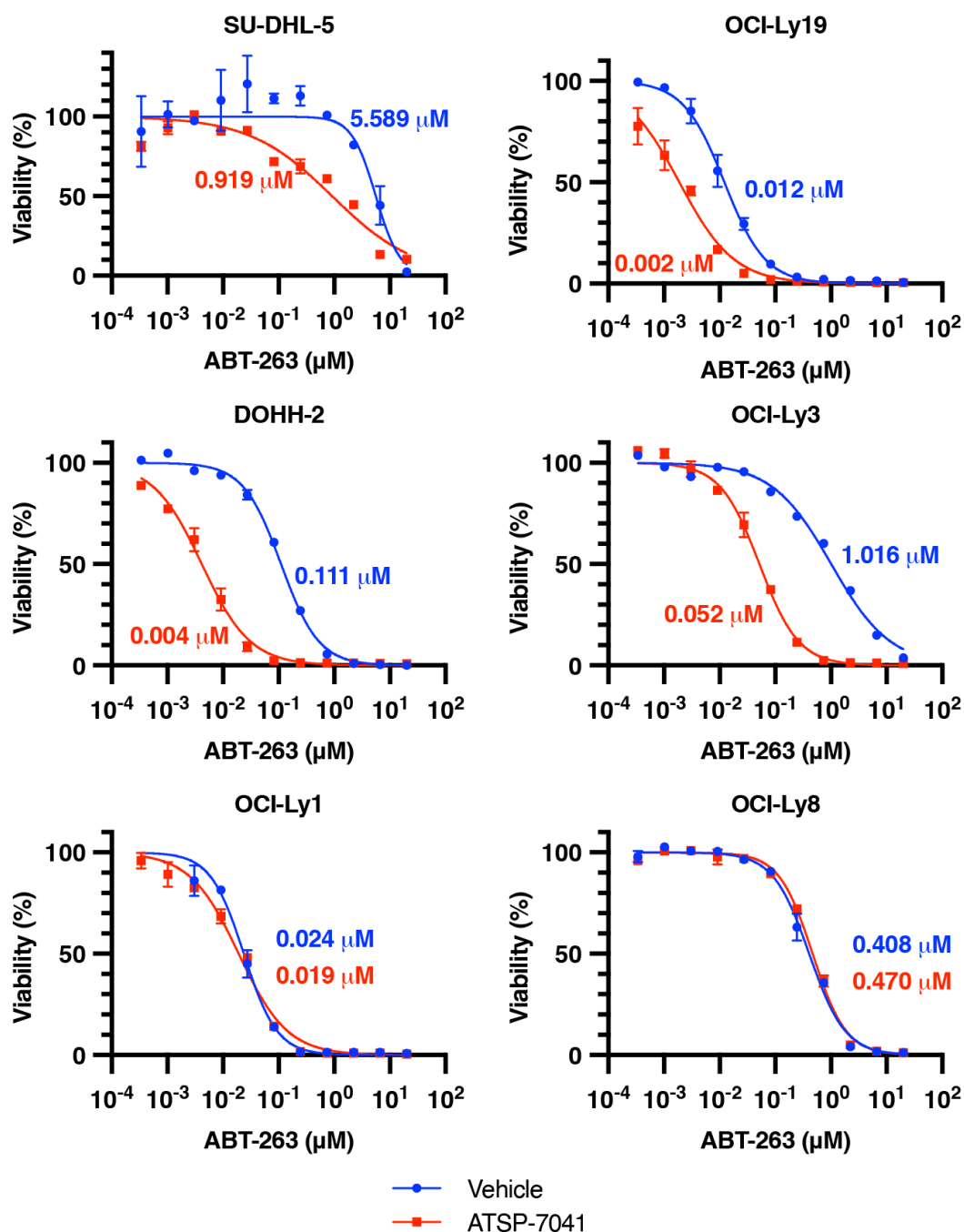


Figure S3: Cell death sensitivity to ABT-263 after priming with ATSP-7041. Cells were treated for 24 hr with ATSP-7041 or vehicle control. Pre-treated cells were then washed and plated with dose titrations of ABT-263, and viability was measured 24 hr later. Data were normalized to untreated cells from the same pre-treatment condition, plotted as the mean of duplicates \pm SEM, and fitted using nonlinear regression. EC₅₀ is shown.

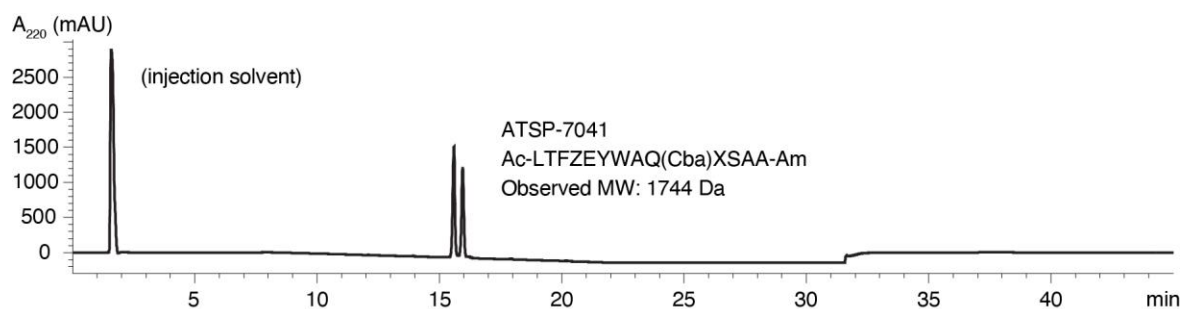


Figure S4: LCMS analysis of purified ATSP-7041. Peptide purity was confirmed by LCMS, integrating the area under the A_{220} curve. Peptide purity was > 95% for each batch. ATSP-7041 eluted as two peaks due to the staple existing as two isomers, as previously reported.⁷¹

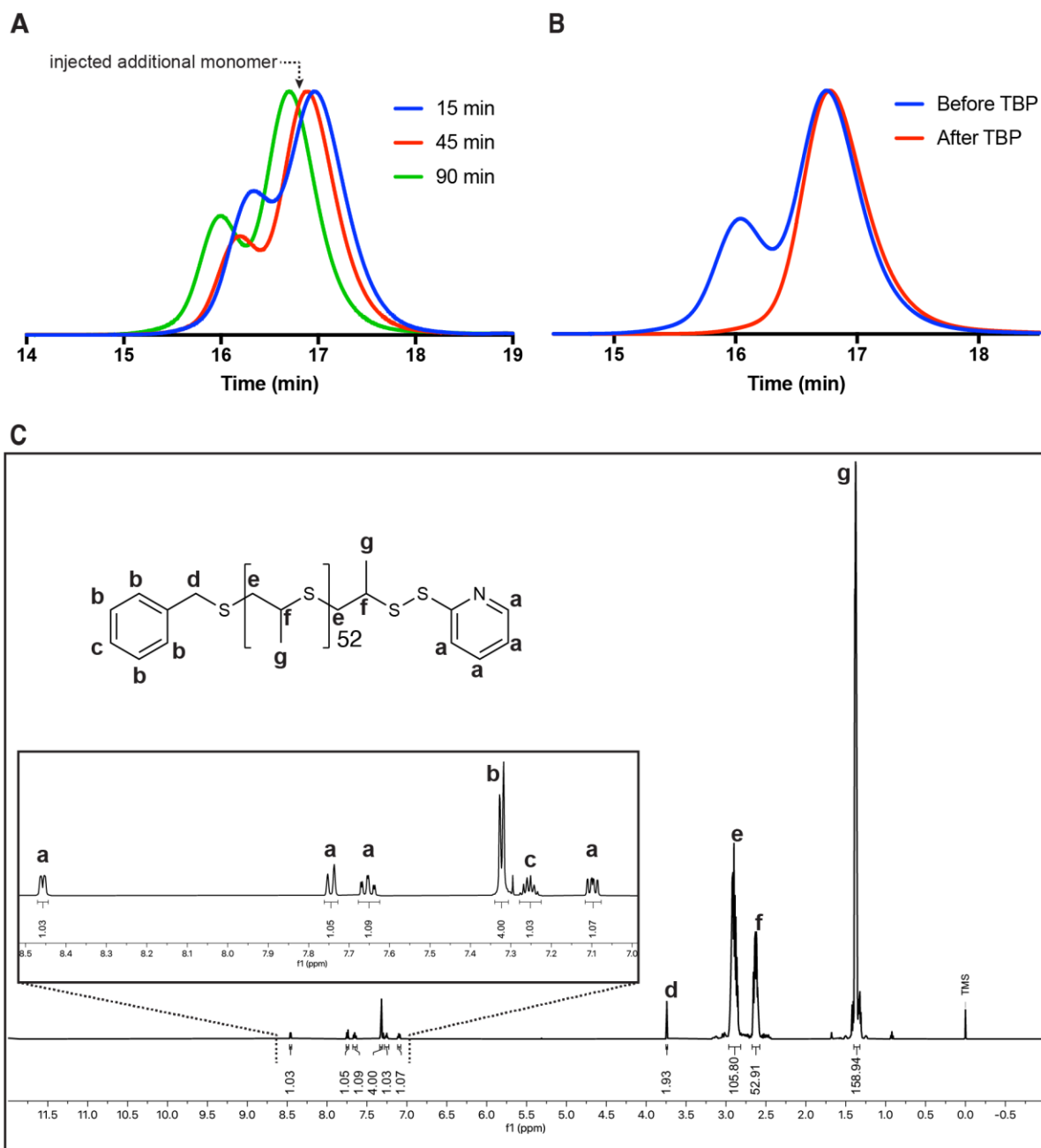


Figure S5: Characterization of PPS-PDS. (A) During PPS-SH polymerization, two peaks were visible by GPC with mobile phase DMF + 0.01 M LiBr at 50 °C, and both peaks grew to larger MW with additional monomer. The larger MW polymer (leftmost peak) was presumably two PPS-SH polymers linked by a disulfide bond. (B) Reduction with TBP eliminated the higher MW peak, reducing disulfide polymers back into PPS-SH. The dispersity of reduced PPS-SH was 1.17. (C) ¹H NMR spectrum of PPS-PDS in CDCl₃.

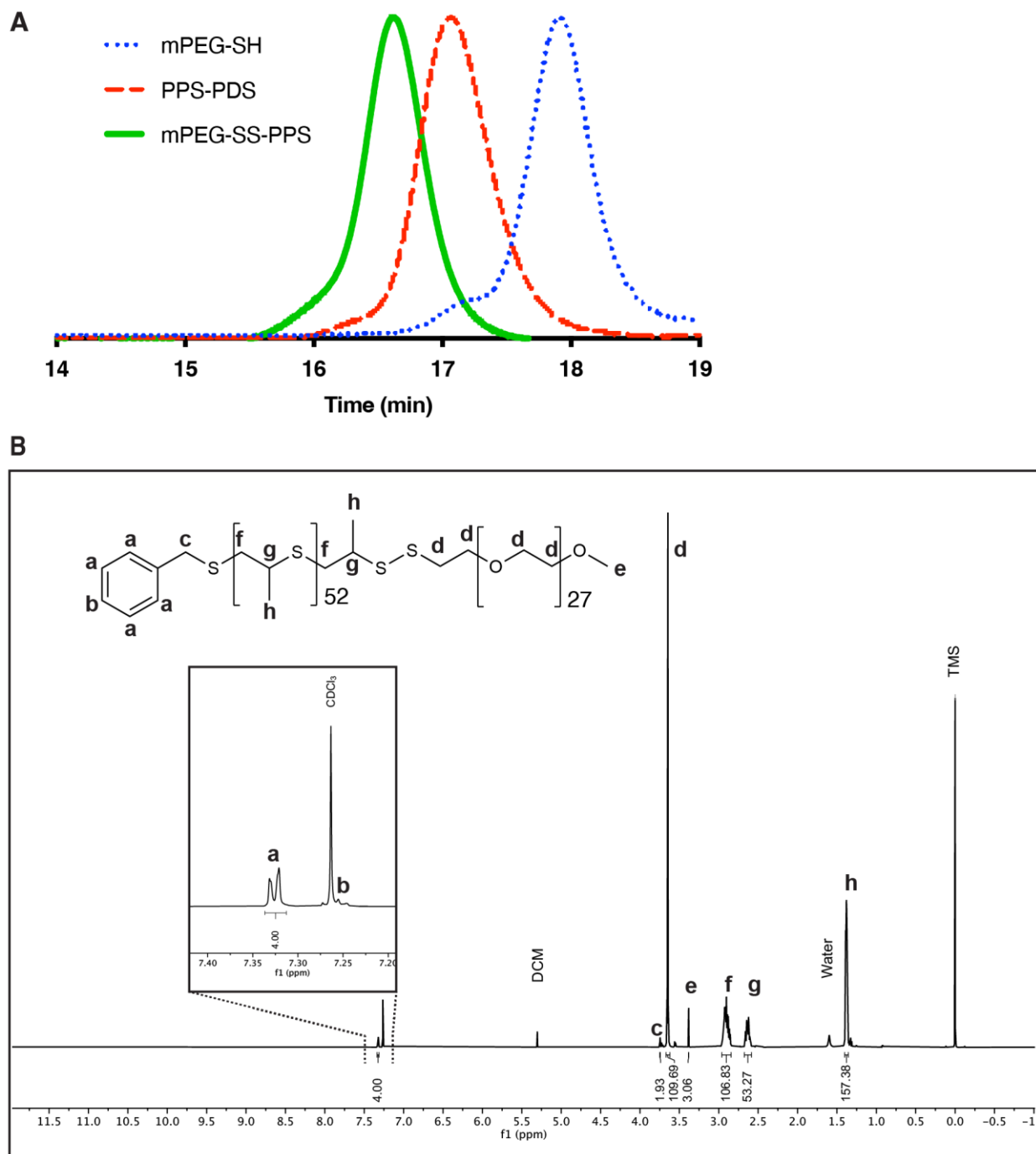


Figure S6: Characterization of mPEG-SS-PPS. (A) Chromatogram of mPEG-SS-PPS (Dispersity = 1.08) and its precursor polymers measuring refractive index via GPC with mobile phase DMF + 0.01 M LiBr at 50 °C. (B) ¹H NMR spectrum of mPEG-SS-PPS in CDCl₃.

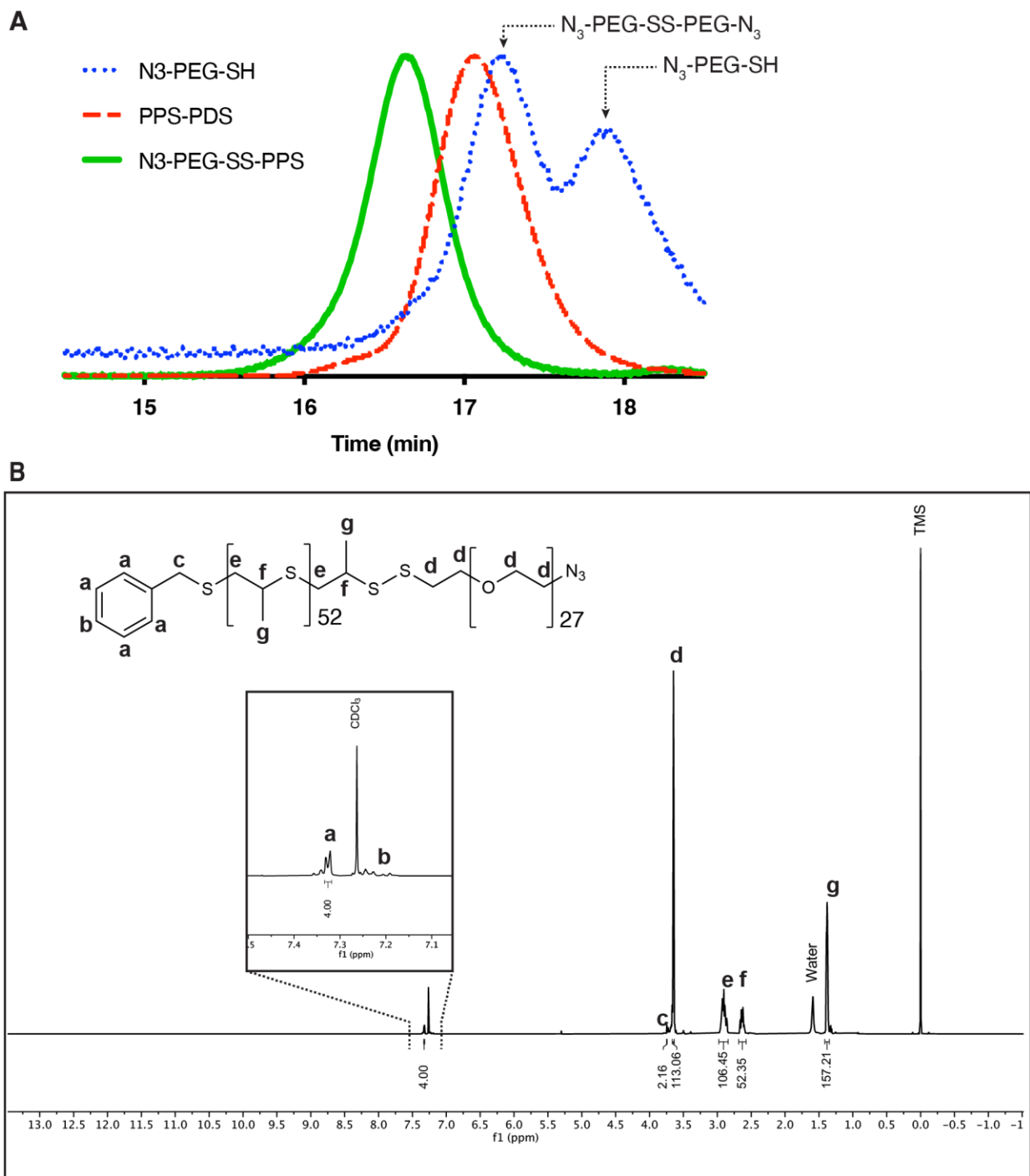


Figure S7: Characterization of $\text{N}_3\text{-PEG-SS-PPS}$. (A) Chromatogram of $\text{N}_3\text{-PEG-SS-PPS}$ (Dispersity = 1.06) and its precursor polymers measuring refractive index via GPC with mobile phase DMF + 0.01 M LiBr at 50 °C. (B) ^1H NMR spectrum of $\text{N}_3\text{-PEG-SS-PPS}$ in CDCl_3 .

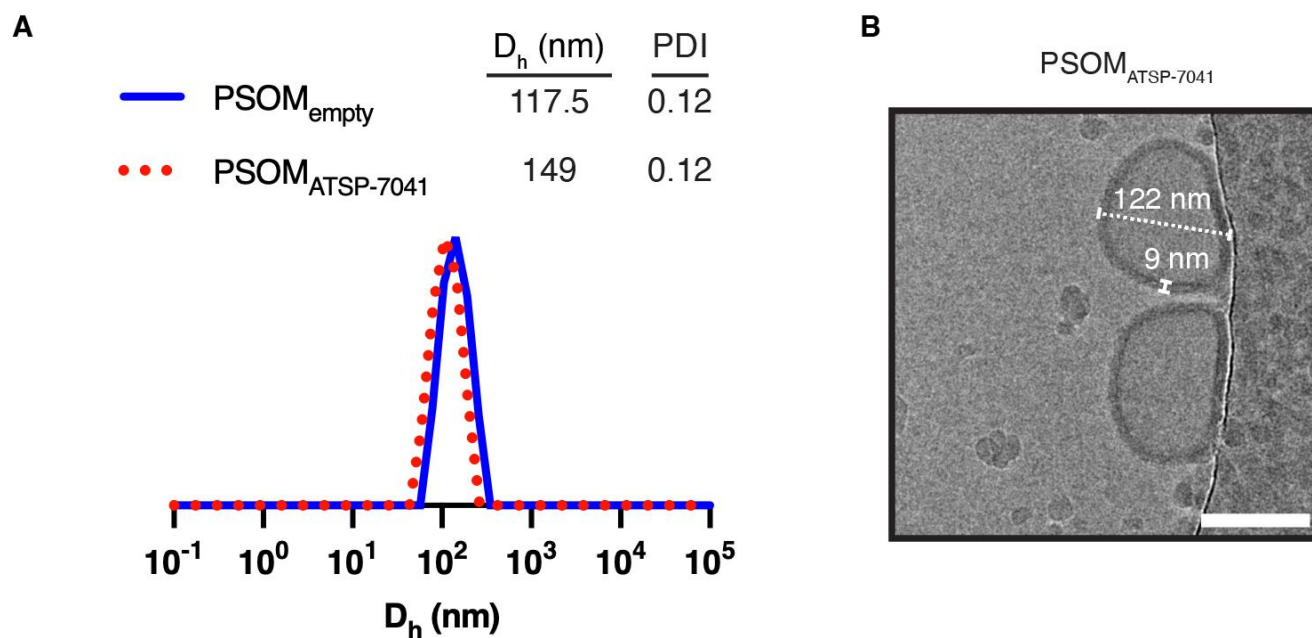


Figure S8: Characterization of PSOM_{ATSP-7041}. (A) DLS measurements of PSOM_{empty} and PSOM_{ATSP-7041} show similar hydrodynamic diameter (D_h). (B) Cryo-TEM confirms that PSOM_{ATSP-7041} forms hollow spheres with diameter and bilayer thickness similar to PSOM_{empty} (Figure 3J). Scale bar is 100 nm.

	Sequence	Translation
V_k	<p>αCD19</p> <p>1 - 30 GATATCTTGCTCACCCAACTCCAGTTCT 31 - 60 TTGGCTGTGTCTCTAGGGCAGAGGGCCACC 61 - 90 ATCTCCTGCAAGGCCAGCCAAAGTGTGAT 91 - 120 TATGATGGTGATAGTTATTGAACTGGTAT 121 - 150 CAACAGATTCCAGGACAGCCACCCAAACTC 151 - 180 CTCATCTATGATGCATCCAATCTAGTTTCT 181 - 210 GGAATCCCACCCAGGTTTGTGGCAGTGGG 211 - 240 TCTGGGACAGACTTCACCCTCAACATCCAT 241 - 270 CCTGTGGAGAAGGTGGATGCTGCAACCTAT 271 - 300 CACTGTGACAAAGTACTGAGGACCCGTGG 301 - 330 ACGTTCGGTGGAGGCCACCAAGCTGGAATC 331 - 333 AAA</p>	<p>1 - 10 DILLTQTPAS 11 - 20 LAVSLGQRAT 21 - 30 ISCKASQSDV 31 - 40 YDGD SYLNNWY 41 - 50 QQIPGQPPKL 51 - 60 LIYDASNLVS 61 - 70 GIPPRFSGSG 71 - 80 SGDTFTLNIH 81 - 90 PVEKVDATY 91 - 100 HCQSTEDPW 101 - 110 TFGGGTKLEI 111 K</p>
	<p>αOspA</p> <p>1 - 30 GATATCAAATGACCCAGAGTCCAAGTAGT 31 - 60 CTTAGTGCCACACTGGGCGGTAAAGTGACG 61 - 90 ATCACTTGAAGGCCAGCCAGGACATCAAC 91 - 120 AAATACATAGCTTGGTATCAGCATAAACCG 121 - 150 GGAAGGGGACCGAGACTGCTGATCCATTAT 151 - 180 ACTTCCACGCTCCAGCCCGGTAAACCAAGC 181 - 210 CGATTTTCTGGGAGCGGAAGTGGTAGGGAT 211 - 240 TATAGCTTTTCCATTAGCAACTTGAAGGCC 241 - 270 GAAGACATTGCTATATACTACTGTCTGCAA 271 - 300 TATGACAACTTGCAGCGCACTTTTGGTGGG 301 - 321 GGAACCAAAGTGAAATTAAG</p>	<p>1 - 10 DIQMTQSPSS 11 - 20 LSATLGGKVT 21 - 30 ITCKASQDIN 31 - 40 KYIAWYQHKP 41 - 50 GKGPRLLIHY 51 - 60 TSTLQPGNPS 61 - 70 RFSGSGSGRD 71 - 80 YFSISINLEA 81 - 90 EDIAIYYCLQ 91 - 100 YDNLQRTFGG 101 - 107 GTKVEIK</p>
	<p>αCD19</p> <p>1 - 30 CAAGTGCAACTCCAACAGTCAGGGGCTGAG 31 - 60 CTGGTGAGGCCTGGCTCCTCAGTGAAGATT 61 - 90 TCCTGCAAGGCTTCTGGCTATGCATTAGT 91 - 120 AGCTACTGGATGAACTGGGTGAAGCAGAGG 121 - 150 CCTGGACAGGGTCTTGTAGTGGATTGGACAG 151 - 180 ATTTGGCCTGGAGATGGTGATACTAACTAC 181 - 210 AATGGAAGTTCAAGGGTAAAGCCACTCTG 211 - 240 ACTGCAGACGAATCTCCAGCACAGCCTAC 241 - 270 ATGCAACTCAGCAGCCTAGCATCTGAGGAC 271 - 300 TCTGCGGTCTATTCTGTGCAAGACGGGAG 301 - 330 ACTACGACGGTAGGCCGTTATTACTATGCT 331 - 360 ATGGACTACTGGGGTCAAGGAACCTCAGTC 361 - 372 ACCGTCTCGAGC</p>	<p>1 - 10 QVQLQQSGAE 11 - 20 LVRPGSSVKI 21 - 30 SCKASGYAFS 31 - 40 SYWMNWWVKQR 41 - 50 PGQGLEWIGQ 51 - 60 IWPFGDGTNY 61 - 70 NGKFKGKATL 71 - 80 TADESSSTAY 81 - 90 MQLSSSLASED 91 - 100 SAVYFCARRE 101 - 110 TTTVGRYYYA 111 - 120 MDYWGQGTSTV 121-124 TVSS</p>
V_H	<p>αOspA</p> <p>1 - 30 CAGATCCAACCTCGTGCACTCTGGACCCGAG 31 - 60 TTGAAGAAACCCGGTGAGACTGTAAAGATT 61 - 90 TCTTGCAAGGCTCCGGCTACACATTTACC 91 - 120 GATTATTCCATGTACTGGGTGAAGCAGGCA 121 - 150 CCTGGAAGAGGGTTGAAAAGGATGGGTTGG 151 - 180 ATAAACACAGAAACCGGCGAACCACCTAT 181 - 210 GCCGACGACTTCAAGGGTCAAGTTCGCGCTT 211 - 240 TCCCTGGATACTTCCGCTCCACCGCATAC 241 - 270 CTTACATTTCCAACCTCAAGAACGAAGAC 271 - 300 ACAGCTACATACTTTTGCGCCGAGGACTT 301 - 330 GATAGCTGGGGTCAAGGTACTAGTGTACC 331 - 339 GTCTCGAGC</p>	<p>1 - 10 QIQLVQSGPE 11 - 20 LKKPGETVKI 21 - 30 SCKASGYTFT 31 - 40 DYSMYWWKQA 41 - 50 PGKGLKRMGW 51 - 60 INTETGEPTY 61 - 70 ADDFKGRFAL 71 - 80 SLDTASTAY 81 - 90 LHISNLKNE 91 - 100 TATYFCARGL 101 - 110 DSWGQGTSTV 111 - 113 VSS</p>
	<p>C_k</p> <p>1 - 30 CGGGCTGATGCGGCGCCAACCTGTATCCATC 31 - 60 TTCCCACCATCCAGTGAGCAGTTAACATCT 61 - 90 GGAGGTGCCTCAGTCGTGTCTCTTGAAC 91 - 120 AACTTCTACCCAAAGACATCAATGTCAAG 121 - 150 TGGAAGATTGATGGCAGTGAACGACAAAAT 151 - 180 GGCGTCTGAAACAGTTGGACTGATCAGGAC 181 - 210 AGCAAAGACAGCACCTACAGCATGAGCAGC 211 - 240 ACCCTCACGTTGACCAAGGACGAGTATGAA 241 - 270 CGACATAACAGCTATACCTGTGAGGCCACT 271 - 300 CACAAGACATCAACTTCAACCATTTGTCAAG 301 - 321 AGCTTCAACAGAAATGAGTGT</p>	<p>1 - 10 RADAAPT VSI 11 - 20 FPPSSEQLTS 21 - 30 GGASVVCFLN 31 - 40 NFYPKIDINVK 41 - 50 WKIDGSEKRN 51 - 60 GVLNSWTDQD 61 - 70 SKDSTYSMS 71 - 80 TLTLTKDEYE 81 - 90 RHNSYTCAT 91 - 100 HKTSTSPIVK 101 - 107 SFNRNEC</p>
	<p>C_H</p> <p>1 - 30 GCCAAACGACACCCCATCTGTCTATCCA 31 - 60 CTGGCCCTGGATCTGCTGCCAAACTAAC 61 - 90 TCCATGGTGACCCTGGGATGCCTGGTCAAG 91 - 120 GGCTATTTCCCTGAGCCAGTGACAGTGACC 121 - 150 TGGAACCTCTGGGTCCTGTCCAGCGGTGTG 151 - 180 CACACCTTCCAGCTGTCTGCGAGTCTGAC 181 - 210 CTCTACACTCTGAGCAGCTCAGTGACTGTC 211 - 240 CCCTCCAGCACCTGGCCAGCGAGACCGTC 241 - 270 ACCTGCAAGCTTGCCACCCGCGCAGCAGC 271 - 300 ACCAAGGTGGACAAGAAATTGTGCCAGG 301 - 312 GATTGCGGATCC</p>	<p>1 - 10 AKTTPPSVYP 11 - 20 LAPGSAAQTN 21 - 30 SMVTLGCLVK 31 - 40 GYFPEPTVT 41 - 50 WNSGSLSSGV 51 - 60 HTFPAVLQSD 61 - 70 LYTLSSTVT 71 - 80 PSSTWPSSTV 81 - 90 TCNVAHPASS 91 - 100 TKVDKKIVPR 101 - 104 DCGS</p>
Cysteine Linker		1 - 8 GGSGSGSGC

Figure S9: DNA coding sequences of α CD19 and α OspA Fabs and their protein translations. Fabs were designed with variable domains (V_{κ} and V_H) for binding to either human CD19 (α CD19) or a xenoantigen control (α OspA). All Fabs shared the same constant domains (C_{κ} and C_H). For α CD19-cys and α OspA-cys, the cysteine linker sequence was added to the C-terminal end of the C_H domain.

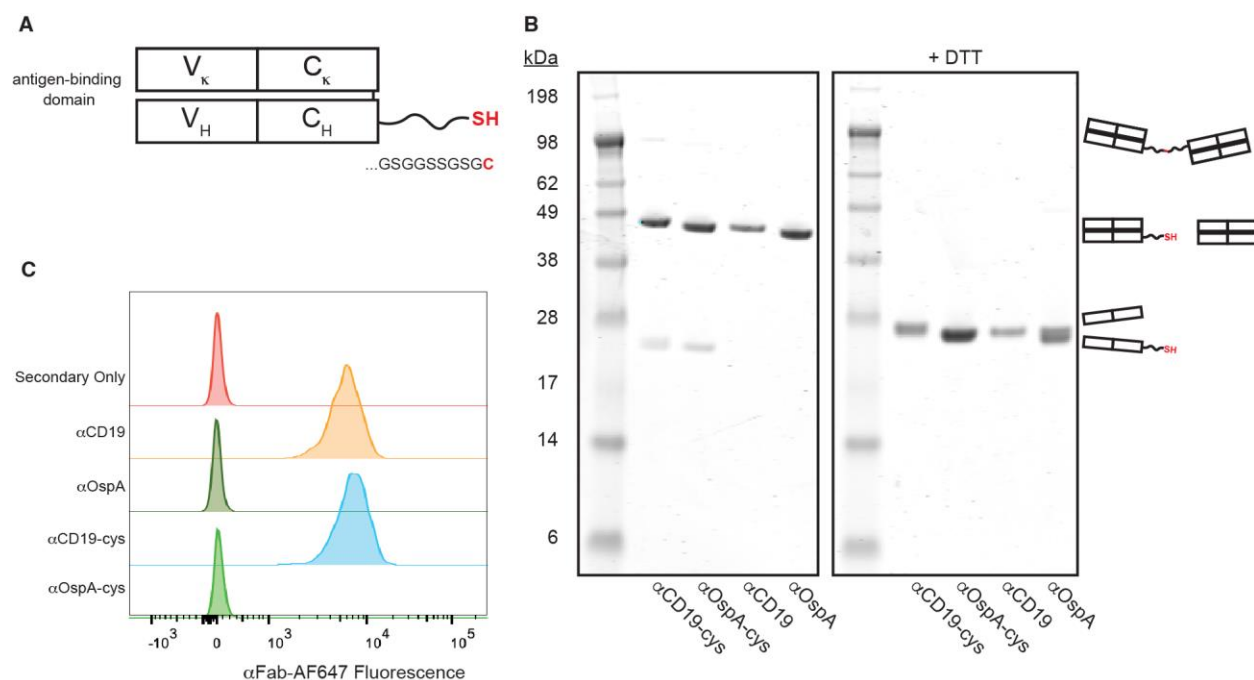


Figure S10: Expression and binding validation of α CD19 and α OspA Fabs. (A) Fabs were designed using previously published sequences from antibodies that bind either human CD19 (α CD19) or a xenoantigen control (α OspA) as described in Materials and Methods.⁷³⁻⁷⁶ To enable site-specific conjugation to polymersomes, a flexible cysteine linker was encoded at the C-terminus of the heavy chain of each Fab to generate α CD19-cys and α OspA-cys. (B) Coomassie-stained SDS-PAGE of purified Fabs. Each Fab appears pure at the expected molecular weights. To confirm proper Fab formation, addition of DTT in the loading buffer reduces the interchain disulfide to generate polypeptides (heavy chain and light chain) that overlap at their expected molecular weights. (C) Flow cytometric measurement of Fab binding to a CD19⁺ DLBCL cell line, SU-DHL-5. Cells were stained with the indicated Fab, followed by an AF647-labeled α Fab secondary antibody. α CD19 Fabs bind CD19⁺ DLBCL with or without the cysteine linker, and the control (α OspA) Fabs do not.

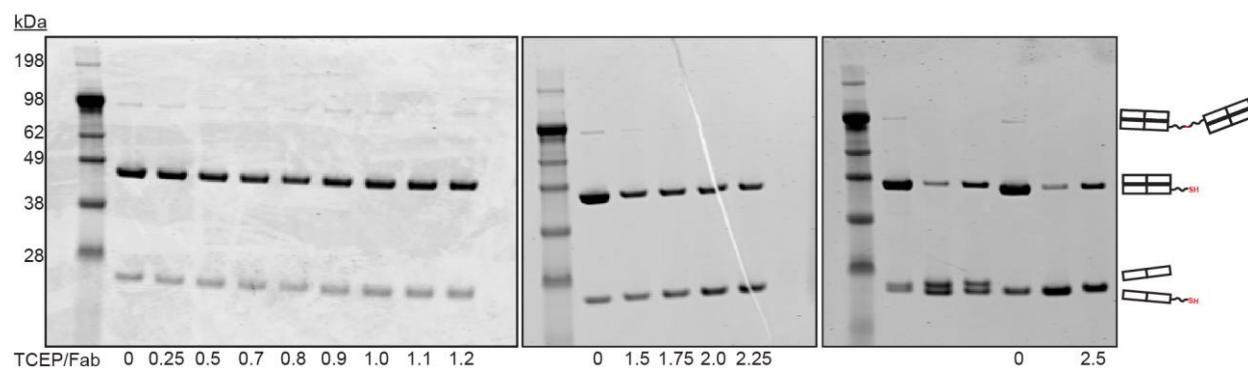


Figure S11: Full Coomassie-stained SDS-PAGE gels from Figure 4C. α OspA-cys was reduced with varying amounts of TCEP, reacted with Sulfo-DBCO-PEG4-Maleimide, purified by desalting, and separated on SDS-PAGE gels. The gels were Coomassie-stained, and the bands in each lane were quantified using ImageJ. Unlabeled lanes contain samples irrelevant to this work.

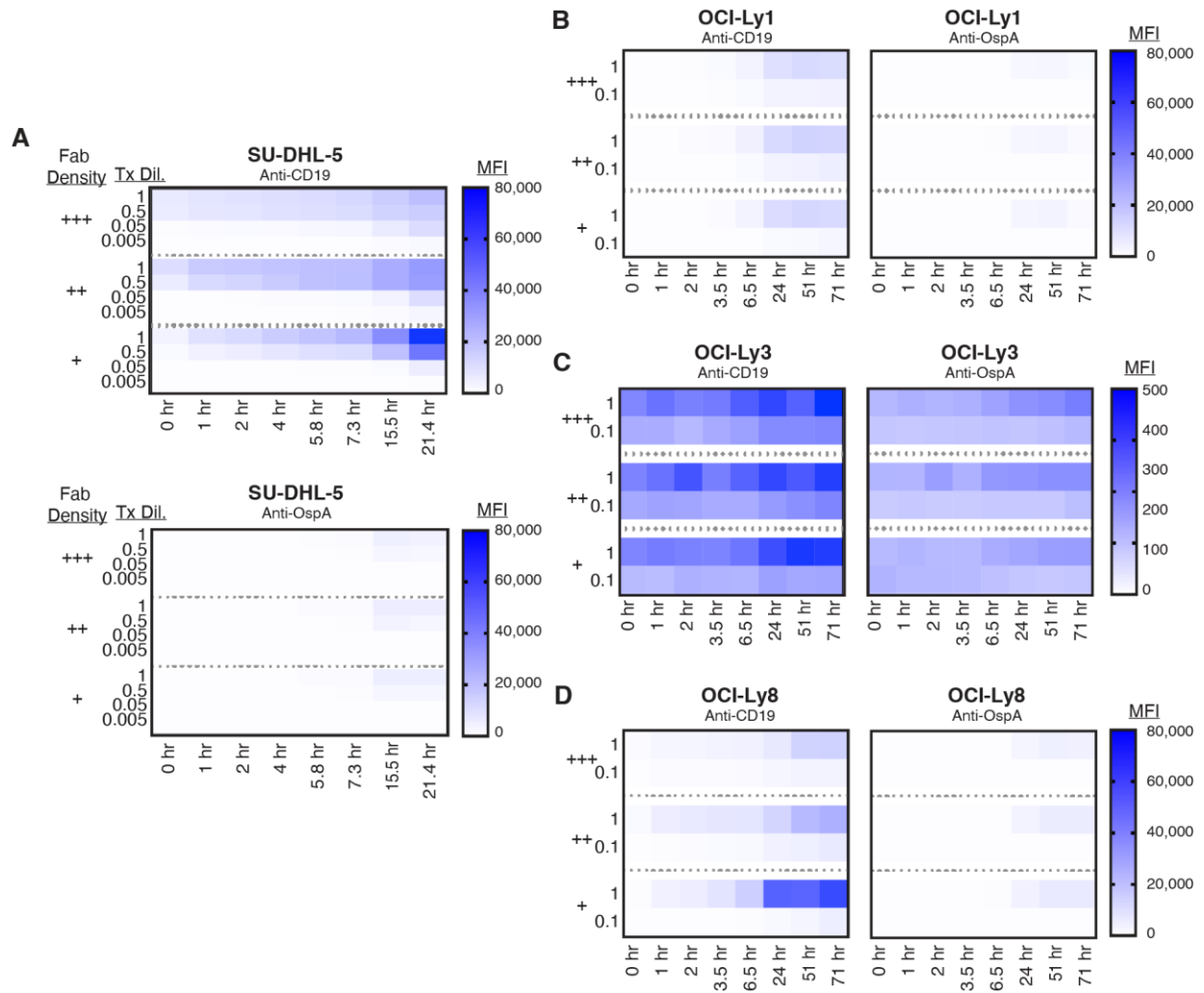


Figure S12: CD19 targeting enhances polymersome delivery of calcein into various DLBCL cell lines. DLBCL cells were treated with CD19-targeted or xenoantigen (OspA) targeted polymersomes loaded with calcein and analyzed by flow cytometry. Treatment concentrations were held constant across samples based on calcein absorbance after Triton X-100 disruption and calcein dequenching. The uptake of fluorescent polymersomes was dependent upon time, concentration, CD19 targeting, and Fab density. α CD19 Fab functionalization greatly improved cellular uptake, and lower Fab densities caused more uptake. This was conducted in **(A)** SU-DHL-5, **(B)** OCI-Ly1, **(C)** OCI-Ly3, and **(D)** OCI-Ly8. The data in (D) are identical to Figure 4E, shown for comparison across cell lines. +++ = 1% theoretical Fab density, ++ = 0.5% theoretical Fab density, + = 0.1% theoretical Fab density.

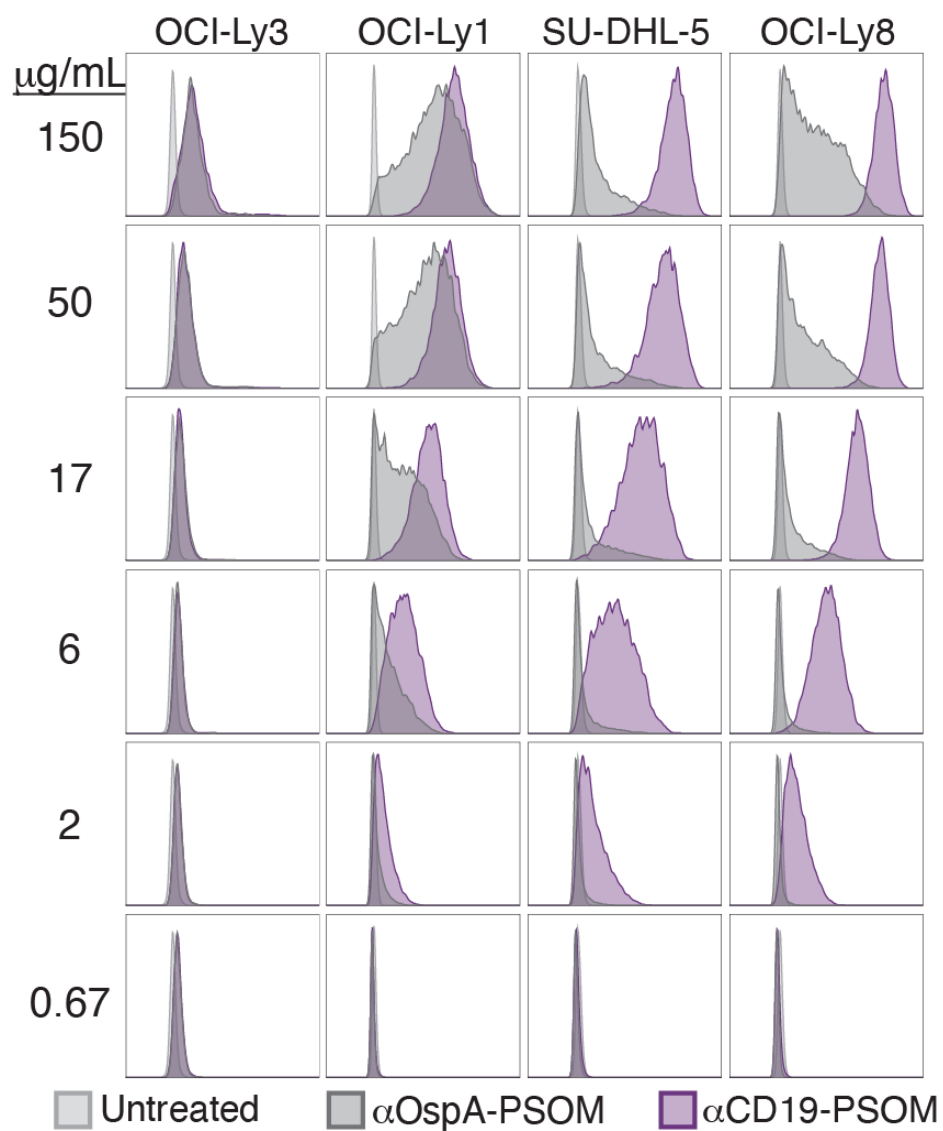


Figure S13: Polymersome uptake into DLBCL cell lines depends upon CD19 cell surface expression and polymersome dose. DLBCL cell lines were treated with calcein-loaded polymersomes for 24 hr and then analyzed by flow cytometry. Both specific uptake/binding (α CD19; purple) and non-specific uptake/binding (α OspA; dark gray) were dose-dependent, but CD19-mediated uptake was significantly greater. The total polymer concentration in each treatment is indicated in $\mu\text{g/mL}$.

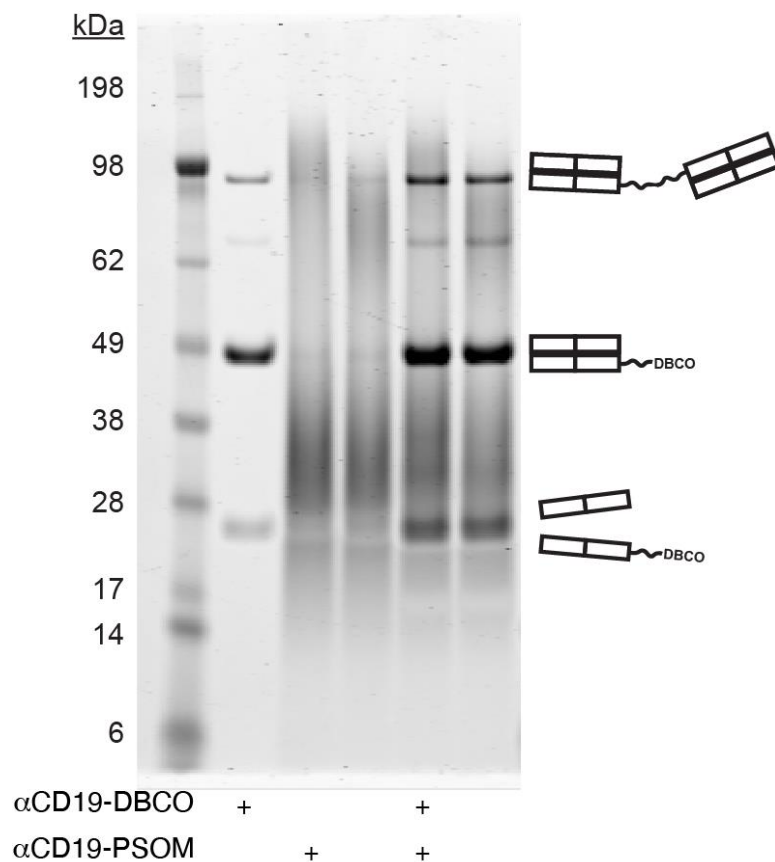


Figure S14: Full Coomassie-stained SDS-PAGE gel from Figure 4H. Bands from Figure 4H are in labeled lanes, and unlabeled lanes contain samples irrelevant to this work. All gel samples were prepared with sodium azide (to quench DBCO:azide reactions) and NEM (to quench thiols and disulfide shuffling). Broad polymer smearing occurred in the presence of sodium azide in the gel samples. Gel samples were loaded such that, assuming 100% Fab conjugation, the Fab bands would be identical. This was calculated using the GPC-measured polymer concentration.

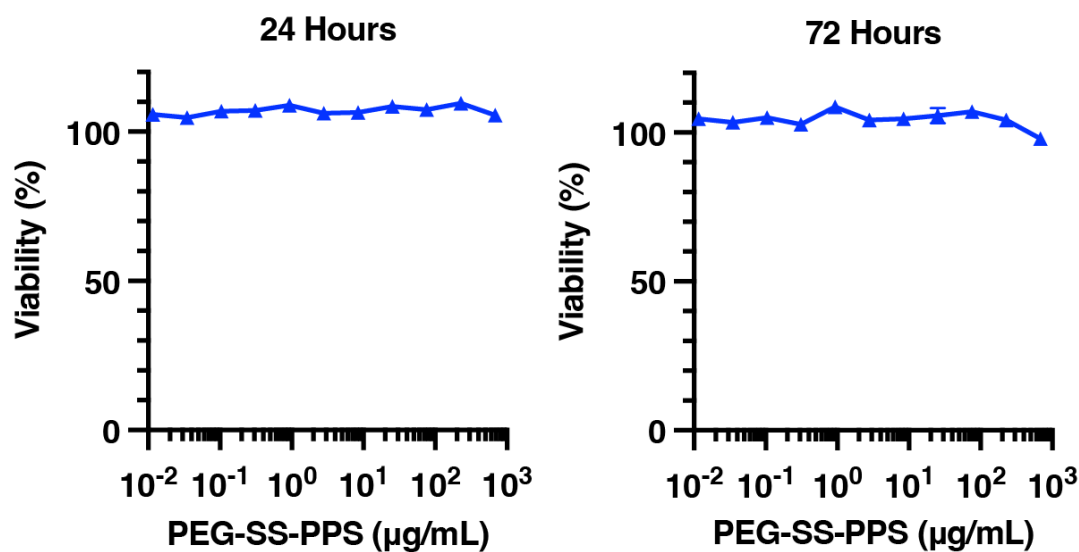


Figure S15: PEG-SS-PPS is non-toxic at high concentrations. OCI-Ly19 cells were treated with α CD19-PSOM_{empty} at varying concentrations of PEG-SS-PPS as high as 682 μ g/mL for 24 hr and 72 hr. No concentration was achieved that inhibited cell viability. Viability was measured using CellTiter-Glo 2.0, normalized to untreated cells, and plotted as the mean of duplicates \pm SEM.

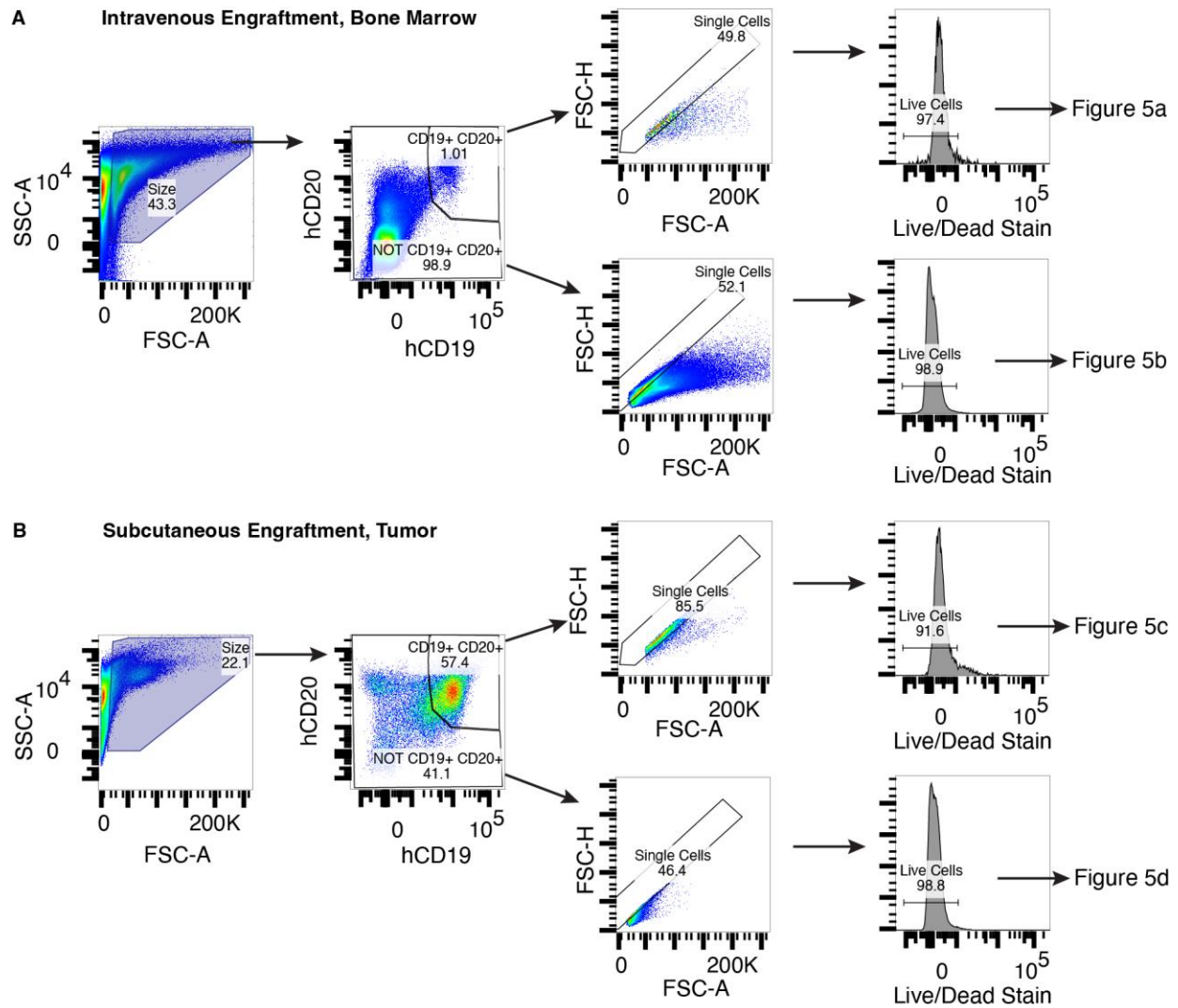


Figure S16: Representative gating strategy for flow cytometry of DLBCL cells from xenografts. After the treatment in Figure 5, (A) bone marrow and (B) subcutaneous tumors were isolated as single-cell suspensions and stained for flow cytometry. Debris was excluded via gating of FSC-A versus SSC-A. DLBCL cells ($CD19^+CD20^+$) were distinguished from other cells in the tissue. The indicated live cell populations were used in Figure 5 to measure fluorescence from mice treated with vehicle or $\alpha CD19$ -PSOM_{calcein}.

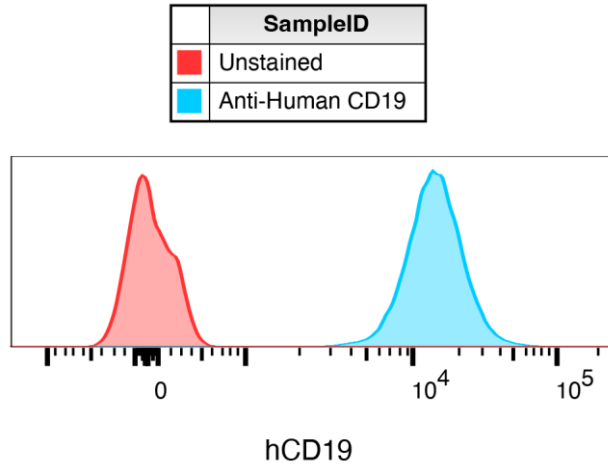


Figure S17: OCI-Ly19 expresses CD19. CD19 expression was measured using flow cytometry after staining cells with an APC-conjugated anti-human-CD19 antibody.

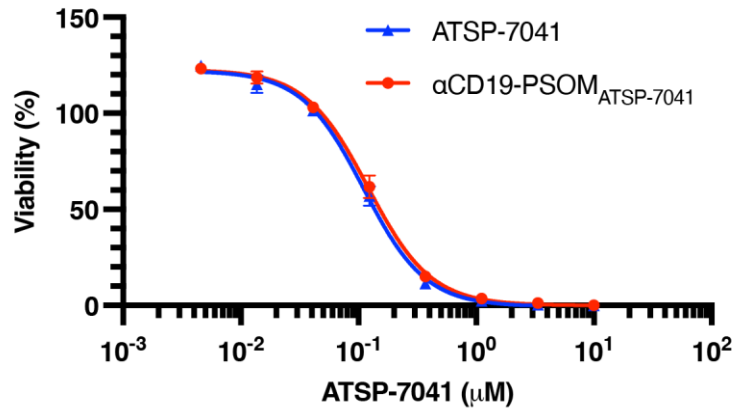


Figure S18: Polymersome delivery maintains the efficacy of ATSP-7041. OCI-Ly19 cells were treated with free ATSP-7041 (blue) or α CD19-PSOM_{ATSP-7041} (red) at varying concentrations of ATSP-7041 for 72 hr. Viability was normalized to untreated cells and plotted as the mean of duplicates \pm SEM.